Available online at www.sciencedirect.com

ScienceDirect

Energy Procedia 45 (2014) 1235 – 1244

Energy Procedia

68th Conference of the Italian Thermal Machines Engineering Association, ATI2013

Experimental and numerical study of a micro-cogeneration Stirling engine for residential applications

Gianluca Valenti[a,*], Paolo Silva[a], Nicola Fergnani[a], Gioele Di Marcoberardino[a], Stefano Campanari[a], Ennio Macchi[a]

[a]*Politecnico di Milano, Dipartimento di Energia, Via R. Lambruschini 4A, 20156 Milano ITALY*

Abstract

Micro-cogeneration Stirling engines are considered promising for residential applications. The present work covers the experimental and numerical analysis of a commercial Stirling unit capable of 8 kW of hot water and 1 kW of electricity. A previously concluded experimental campaign that focused on external measurements is extended here to include internal measurements. The scope is collecting useful data to validate a detailed numerical model. Three test cases are considered by fixing the temperature of the cogeneration water at the unit inlet at alternatively: 30, 50 and 70°C. Mass flow rate of the water is kept at the nominal value of 0.194 kg/s. This numerical model is an extension of the well-known work by Urieli and Berchowitz. The model is calibrated on the 50°C case and compared in the other two cases. Maximum deviations with respect to experiments are about 4% on net power output, whereas they remain below 1% on heat input and rejection. The Stirling unit has shown an electrical efficiency exceeding slightly 9% and a thermal efficiency of 90% (both based on the Higher Heating Value) if the cogeneration water inlet temperature is 30°C, which decreases down to about 84% with water inlet at 70°C. The Primary Energy Index is remarkably positive for all cases, ranging from 17% to 22% as the temperature of the water inlet goes from 70°C to 30°C.

Keywords: Stirling engine; experimental campain; numerical model.

* Corresponding author. Tel.: +39-02-2399-3845; fax: +39-02-2399-3913.
E-mail address: gianluca.valenti@polimi.it

doi:10.1016/j.egypro.2014.01.129

1. Introduction

Micro-cogeneration Stirling engines are considered promising for residential applications primarily because of (i) their high total efficiency, (ii) favorable ratio of thermal to electrical power, similar to a typical heat-to-electricity demand ratio of a domestic load, and (iii) low emissions with respect to alternative technologies, like internal combustion engines, allowed by their external and stationary combustion process. The present work covers the experimental and numerical analysis of a commercial Stirling unit capable of generating 8 kW of hot water (that can be boosted to 15 kW with an auxiliary burner) and 1 kW of electricity operating on natural gas.

As a continuation of a previous investigation accomplished under the support by *Regione Lombardia* [1], a new experimental campaign is carried out at the Laboratory of Micro-Cogeneration of the Department of Energy at Politecnico di Milano in order to collect measurements both internally and externally of the unit under testing and to use these data to validate a numerical model of the unit itself.

The present work describes the experimental activity outlying the setup and the test cases. Afterward, the numerical model is described outlying the mathematical model adopted for the simulation and the input. Ultimately, the results from the experimental campaign and those from the numerical model are compared and discussed in order to draw the conclusions.

2. Experimental campaign

The Laboratory of Micro-Cogeneration (LMC) has been constructed for conducting various types of testing on diverse energy systems of relatively small sizes. Systems can be cogeneration units, also known as Combined Heat and Power (CHP) units, fueled by natural gas, hydrogen, synthetic gas or any mixtures of the previous, and characterized by an electric power production up to 100 kW_{el} and a thermal recovery to 300 kWt_h. The laboratory can also test trigeneration systems, or Combined Cooling Heating and Power (CCHP) systems, that adopt thermal absorption chillers, heat pumps, or boilers. In addition, tests cover electrolyzers and fuel processors for hydrogen production. The laboratory is designed to simulate most plausible operating conditions, by changing independently the flow rates and temperatures of water circuits, the flow rate and the chemical composition of the fuel gas supply, the temperature of the ambient air and the electric load (in terms of voltage, frequency and power factor) [2].

2.1. Setup and instrumentation

As anticipated, the measuring setup comprises measurements that are taken both externally and internally of the engine itself. The external data, recorded at the unit boundary, include the following variables: natural gas molar composition, flow rate, temperature and pressure; ambient air temperature, relative humidity and pressure; water mass flow rate, inlet and outlet pressures and temperatures; exhaust gas molar composition, temperature and emissions; condensate water weight over time; net electric power.

On top of those measurements, a number of temperatures are taken within the engine along the exhaust line, water loop and engine walls, as shown in Figure 1. On the air side, the thermoresistance A3 measures the temperature at the inlet of the engine after pre-heat; on the other side, the probes A7 and A8 show the cooling of the exhaust. Another important measure is given by the thermocouple A5 placed in contact with a vane piston crown that indicates the highest temperature value of the Stirling cycle. All the probes marked with the letter "T" allow determining heat exchanges in the four main steps of the water loop, as described in the next chapter. Finally, the thermocouples from S1 to S4 are placed on the engine walls in order to evaluate the thermal losses.

The experimental data of all tests are statistically filtered and used to reconstruct the mass and energy balance of the unit as well as to calculate the net electrical and thermal efficiency. The employed instrumentation and protocol as well as the elaboration of the data are detailed in the previous work [1]. The collected information is expected to be a useful extension of the data published by Gedeon and Wood [3], who performed an extensive work at NASA facilities, and by Aliabadi et al. [4].

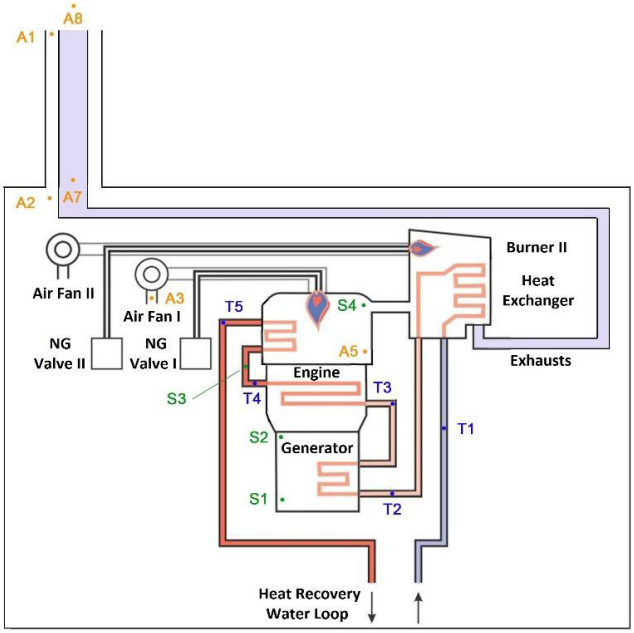

Figure 1. Stirling engine: heat recovery loop and internal measurement setup

2.2. Tests

The free external parameters of the tests are in general the cogeneration water mass flow rate and its temperature at engine inlet. As in the previous characterization work [1], three temperature levels are adopted: 30, 50 and 70°C, while for simplicity water flow rate is kept at the nominal value of 0.194 kg/s. Thus, three test cases are investigated for the purposes of a preliminary validation of the numerical model. Further validation will be performed in the future through additional cases, investigating the effect of internal parameters such as average working fluid pressures and fluid type.

3. Numerical model

The experimental study of the actual thermodynamic phenomena inside the engine, such as instantaneous temperatures and velocities, is a very difficult task because of the presence of fast oscillating flows. The high temperatures of the heater make the task even more complex. An accurate numerical model turns useful to evaluate the major sources of energy waste and to optimize the geometries of both the engine and the heat exchangers.

Among the many numerical methods reported in the literature, many of which are listed by Chen and Griffin [5] or by Cullen and McGovern [6], the first attempt was likely conducted by Finkelstein [7]. Then were Shultz and Schwendig [8] to build the first simulation model of the general Stirling cycle. This model was subsequently optimized by Kongtragool and Wongwises [9], who added the effects of dead volumes. Later on several studies were performed, among which the most remarkable are those by Karabulut on Beta free piston engines [10], by Parlak [11] on Gamma engine under almost stationary flow conditions, and by Andersen on a one-dimensional model [12]. The first Computational Fluid Dynamics (CFD) models were realized by Organ [13] and Mahkamov [14]. A fundamental contribution was given definitely by Urieli and Berchowitz in 1977 [15]. Their numerical model, especially in the so-called variant “simple analysis”, represents a good compromise between simplicity and accuracy for the calculation of the performances of the engine, while subsequent modeling evolutions reported in literature are mainly dedicated to specific engine configurations and component analysis.

3.1. Structure of the numerical model

The numerical model developed in this study is a modification of the well-known Urieli and Berchowitz work. The engine is divided into five different cells, as visualized in Figure 2. From left to right, the cells are: (i) fluid compression, (ii) cooling, (iii) regeneration, (iv) heating, and (v) expansion. The model comprises in sequence:

- splitting one engine cycle in to short steps (e.g. 10° of shaft revolution);
- studying the thermodynamic conditions inside each cell and for each step;
- studying gas transfer flow between neighboring cells and heat/work exchanged though the walls/pistons of the engine for each step;
- integrating the cited head/work exchanged over one shaft revolution to evaluate the performances of the engine (e.g. heat power input, mechanical power transferred to the shaft, heat rejected to the cooler).

Moreover, the thermodynamic processes inside the compression and expansion cells are assumed to be adiabatic, while the temperatures inside the cooling and heating cells are assumed to be uniform within each step.

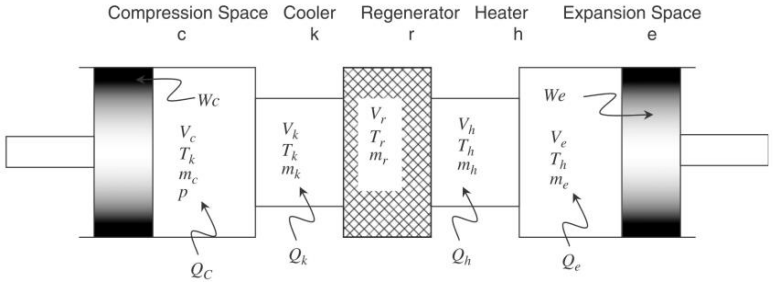

Figure 2. Scheme showing the five cell that are at the base of the mathematical model of the engine

With respect to the original model, the present one includes several novel subroutines aiming to predict the following parameters: (i) thermal behavior of the metal screen regenerator under oscillating flow conditions; (ii) irreversibility of exchanged heat within the cells of heater and cooler; (iii) concentrated and distributed pressure losses within the cells of heater, cooler and regenerator; (iv) heat losses due to conduction from the heater to the cooler, through the iron walls. Among these, the thermal performance of the regenerator is the most critical in terms of reduction of the total efficiency. In fact, the performance of such a component is not easy to be evaluated because most of the studies relating to the heat exchange phenomena reported in the literature refer to steady-flow conditions that are well away from the real oscillating flow conditions. However, the experimental work by Gedeon and Wood [3] provides correlations for the calculation of thermal performance and pressure drops inside the regenerator as functions of several physical parameters. These correlations are implemented in the present model.

The non-ideality of the exchanged heat inside the heater and the cooler yields a decrease of gas temperature inside the heater, along with an increase of gas temperature inside the cooler, for a given set of wall temperatures. The temperature differences between gas and walls are evaluated, step by step, by means of heat exchange coefficients, assuming forced convection conditions inside the ducts.

The prediction of heat exchange phenomenon and temperature evolution inside the engine is based on gas speed and pressure, which are obtained through a preliminary simulation. The non-ideal exchanged heat strongly affects the actual thermodynamic cycle followed by the engine and varies the previously calculated speeds and pressures. A few iterations are therefore necessary in order to reach a stable solution, as reported in Figure 3.

By the point of view of pressure drops the most critical component is the regenerator due to the great extension and tortuosity of the exchange surface. The losses generated by the friction of fluid flow, called pumping losses, have a direct effect in terms of reducing the cycle useful work. Conceptually the frictional losses occurring in the cooler and in one semi-volume of the regenerator cause an increase in compression work, while those occurring in the heater and in the other semi-volume of the regenerator cause a reduction of expansion work. Moreover, the work dissipated due

to pumping losses causes an additional heating of the working fluid, which reduces the heat that must be introduced through the heater and increases the one that must be removed through the cooler.

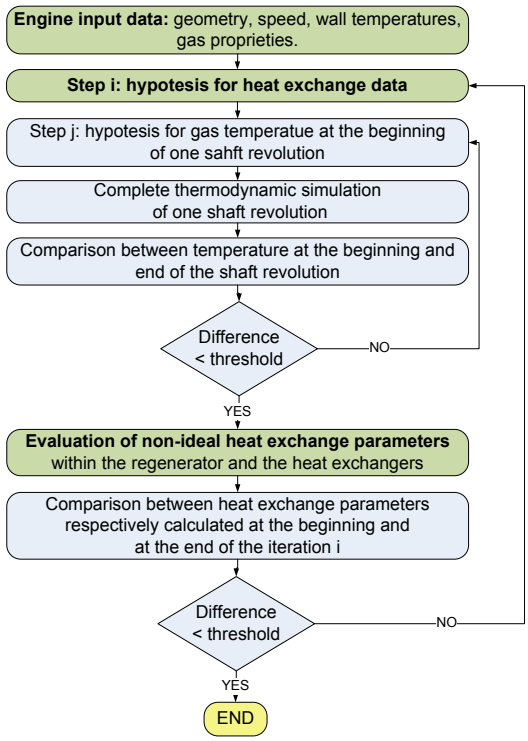

Figure 3. Flow diagram of the algorithm developed to solve the numerical model

3.2. Input data

The model analyses the behavior of a single compressor-cooler-regenerator-heater-expander volume, while the engine is made up by four cylinders arranged on a circular disposition. Input data include the complete geometry of the engine and of the heat exchangers, the composition and nominal pressure of gas, the operating temperatures and the shaft speed. Table 1 shows the set of input data used in the simulations. The geometry is defined according to the direct measurements of few parts of the engine and to hypothesis regarding the inaccessible parts. These data remain constant for every simulation, while the cooler temperature is varied according to the experimental campaign.

3.3. Results of the simulation

Once convergence is reached, the model allows calculating the mass and energy balance occurring in every cylinder during one shaft revolution. Moreover, it allows investigating several thermodynamic parameters evolving within the engine during the cycle, along with the most relevant energy dissipations that affect the engine electrical efficiency. Table 2 reports an example of the non-ideal behavior of heat exchangers, for an experimental set with 50°C cooling inlet water temperature.

The gas-wall temperature difference inside the heater is almost twice as much that inside the cooler. This difference is primarily due to the greater heat flow in the first component as compared to the second one. Secondly, the greater density of the fluid passing through the cooler, along with the presence of smaller sized ducts, results in a greater convective coefficient. It is also noted that the axial conduction losses through the regenerator walls cause a high thermal loss, due to the great temperature difference between cooler and heater.

Table 3 shows the results from the analysis of the losses due to pressure drops. These losses take place in the connection conduits between the different sections of the engine, in the heat exchangers and in the regenerator.

Table 1. Numerical values of the input data for the simulation. Data are related to a single working volume (compressor-cooler-regenerator-heater-expander), i.e. a single cylinder among the four cylinders of the engine.

Engine		**Regenerator**	
type	wobble joke	type	annular
compression space clearance volume [cm^3]	19.1	external annulus outer diameter [m]	0.0636
compression space swept volume [cm^3]	27.4	external matrix diameter [m]	0.0566
expansion space clearance volume [cm^3]	19.9	internal matrix diameter [m]	0.0435
expansion space swept volume [cm^3]	28.4	internal annulus inner diameter [m]	0.0415
Wobble joke arm length [m]	0.0725	length [m]	0.02
cylinder stroke [m]	0.021	matrix type	porous media
expansion space phase angle advance [deg]	90	porosity	0.698511
gas type	Nitrogen	wire matrix diameter [m]	6.00E-05
cold engine average pressure [Pa]	2.00E+06	total matrix wet surface [m^2]	0.35
Cooler / heater wall temperature [K]	406.7 / 823	matrix screen width [m]	0.000216
Engine speed [Hz]	25	number of cross section wires	6367
Cooler		**Heater**	
type	fins	type	fins
length [m]	0.052	length [m]	0.049
number of fins	180	number of fins	84
fins height [m]	0.0018	fins height [m]	0.003
fin-to-fin width [m]	5.55E-04	fin-to-fin width [m]	5.00E-04
cooler average cross section [m^2]	1.80E-04	heater average cross section [m^2]	1.26E-04
sum of cooler concentrated loss factors	4	sum of heater concentrated loss factors	4

Table 2. Heat exchange results for the 50°C case (4 cylinder engine).

Regenerator	
Regenerator heat losses	868.8 W
Wall conduction heat losses	1978 W
Cooler	
Cooler wall temperature	51.8 °C
Average gas temperature inside cooler	72.7 °C
Average gas-wall temperature difference	20.9 °C
Heater	
Heater wall temperature	550 °C
Average gas temperature inside heater	507.5 °C
Average gas-wall temperature difference	42.5 °C

Table 3. Pressure drop results for the 50°C case.

Pressure drop	
Average cooler	2425 Pa
Average regenerator	8209 Pa
Average heater	6196 Pa
Pumping loss	
Average cooler	16.4 W
Average regenerator	41.6 W
Average heater	41.6 W
Total	99.6 W

Pumping losses are as low as 7.5% of the 1324 W mechanical gross power output resulting from the simulation (Table 4), mainly due to the low gas speed in all the sections of the engine. The numerical model also allows studying several thermodynamic parameters evolving within the engine during the cycle, such as: gas temperatures and speeds, Reynolds numbers, heat exchange coefficients, pressure drops. In the following graph it is shown an example of pumping losses evolution (in terms of reduction of avaiable work) during the cycle.

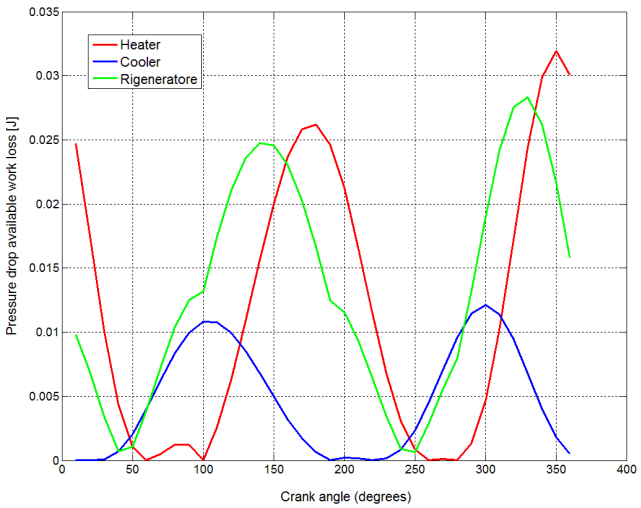

Figure 4. Example of energy due to pumping loss during the cycle

4. Comparison of experimental and numerical results

The comparison of experimental and numerical results is performed to: (i) validate the numerical model and (ii) compare the performance of the engine under different working conditions (i.e. change of cooler temperature). To achieve the scope, it is necessary to isolate the heat flows related to the Stirling engine from those related to the whole CHP unit. There are several heat flows that are directly transferred from the exhausts to the water or to the ambient without being used by the engine. They are:

- exhausts to water heat through the exhausts heat exchanger,
- exhausts to water heat through the cooling annulus of the combustion chamber,
- exhausts to water heat through the walls of the engine,
- exhausts and water heat to combustion air through the walls of the engine,
- exhausts and water heat to the ambient through the walls of the CHP unit.

The complete scheme of heat and power fluxes within the CHP unit, including the ones inside the Stirling engine, is presented in Figure 5.

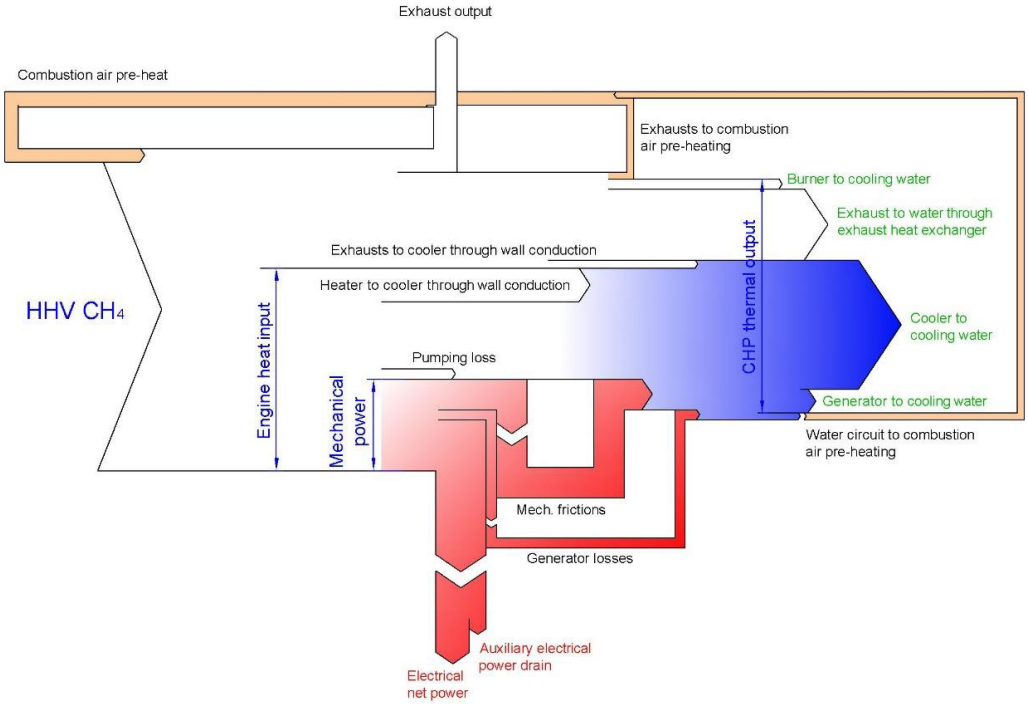

Figure 5. Sankey diagram for heat and power fluxes inside the whole CHP, including the ones of the Stirling engine.

The whole thermal, mechanical and electric power balance of the CHP unit is calculated starting from the experimental data, for the three different values of cooler temperatures. For each experimental set a numerical simulation is performed and the results are compared in Table 4.

It is noted that the net electrical power output, and thus the net electrical efficiency of the engine and of the CHP unit, vary for different inlet water temperatures. Indeed that temperature strongly affects the cooler average temperature, which represents the cold sink of the thermodynamic cycle and was found to be around 5°C higher than the water temperature at the inlet of the cooler.

The data resulting from the experimental set with a water inlet temperature of 50°C is used to calibrate the numerical model. The 50°C set is hence the one that presents the better match between numerical and experimental data. The main differences among the different experimental sets can be observed for the net electrical power output: the numerical model predicts a stronger dependence upon inlet water temperature that it was experimentally observed. This phenomenon could be related to the simulation hypothesis of a constant heater wall temperature for every cooler temperature. Since it is not easy to directly measure this temperature, it can be deduced that the regulation of the natural gas burner in the CHP unit and the variations of the engine cold-side temperatures bring about a reduction in heater wall temperature when the inlet water temperature increases.

The values related to the thermal fluxes inside the engine are not measured and are listed only for numerical simulations, while the energy balances of the whole CHP unit are not studied in the numerical model but are reported only for the reconstruction from experimental data. All the efficiencies are referred to the Higher Heating Value (HHV) of the input natural gas. Measured CHP thermal efficiencies are very high due the high efficiency of the exhausts heat recovery, which permits to achieve the condensation of most of the vapor contents. Regarding the experimental set with 30°C inlet water temperature, the total efficiency is close to unity due to an exhaust gas temperature very close to the ambient temperature (30°C).

The analysis of the mechanical power for the 50°C simulation set shows that the mechanical friction, electro-mechanical conversion and auxiliary power absorption yields a reduction of efficiency, related to the heat input to the Stirling engine (detailed in Table 4 and in Figure 5), from 21.3% (gross mechanical output) to 15.1% (net electrical output). When referring to the fuel input, due to the presence of heat fluxes directly transferred from the exhausts to the water or to the ambient without being used by the engine (Figure 5), the net electrical efficiency of the CHP unit results in the lower value of 9.7%, related to the HHV of the input natural gas. The net electrical measured output is 930 W, very close to the simulated value of 941 W and to the design value of the CHP unit (1000 W).

Table 4. Comparison of experimental and numerical results (Sim. stands for simulation, Exp. experimental, Diff. difference).

Energy balances of engine and CHP unit	**Water inlet 30°C**			**Water inlet 50°C**			**Water inlet 70°C**		
	Sim.	**Exp.**	**Diff.**	**Sim.**	**Exp.**	**Diff.**	**Sim.**	**Exp.**	**Diff.**
Heat input to Stirling engine [W]	6290	6297	0.1%	6227	6188	-0.6%	6152	6158	0.1%
Heat rejected from the cooler [W]	4868	4915	1.0%	4876	4856	-0.4%	4879	4888	0.2%
Heat loss due to piston stroke [W]	172	-	-	165	-	-	157	-	-
Heat loss due to wall conduction [W]	1725	-	-	1654	-	-	1573	-	-
Pumping loss [W]	103	-	-	105	-	-	100	-	-
Heat loss due to non-ideal regenerator [W]	768	-	-	736	-	-	699	-	-
Gross mechanical power [W]	1406	-	-	1324	-	-	1226	-	-
Mechanical frictional loss [W]	225	-	-	212	-	-	196	-	-
Generator energy loss [W]	118	-	-	111	-	-	103	-	-
Auxiliary power absorption [W]	60	-	-	60	-	-	60	-	-
Net electrical power output [W]	1003	964	-4.1%	941	930	-1.2%	867	900	3.7%
Heat transferred to the ambient [W]	-	16	-	-	28	-	-	46	-
Engine net electrical efficiency (%)	15.9%	15.3%	-4.2%	15.1%	15.0%	-0.5%	14.1%	14.6%	3.6%
Heat input to CHP unit (HHV) [W]	-	10077	-	-	9573	-	-	9557	-
Thermal output from CHP unit [W]	-	9082	-	-	8033	-	-	8009	-
Thermal efficiency of CHP unit (HHV, %)	-	90.1%	-	-	83.9%	-	-	83.8%	-
Net electric efficiency of CHP unit (HHV, %)	-	9.6%	-	-	9.7%	-	-	9.4%	-
Total efficiency of CHP unit (HHV, %)	-	99.7%	-	-	93.6%	-	-	93.2%	-

The engine performance can be evaluated by the Primary Energy Index (PES), which is defined accordingly to the EU Directive [16]:

$$PES = 1 - \frac{1}{\frac{\eta_{\mathrm{el,cog}}}{\eta_{\mathrm{el,ref}} \times \mathrm{p}} + \frac{\eta_{\mathrm{th,cog}}}{\eta_{\mathrm{th,ref}}}} \times 100\% \tag{1}$$

where the reference efficiencies for the separate generation of electricity and heat, $\eta_{el,ref}$ and $\eta_{th,ref}$, are taken to be 52.5% and 90%, based on the Lower Heating Value (LHV) of the fuel, reflecting the Italian implementation of the directive for the case of CHP units fuelled by natural gas. For the sake of simplicity, the grid efficiency coefficient, p, is conservatively equal to unity. The efficiency values for the Stirling engine in Eq. 1, $\eta_{el,cog}$ and $\eta_{th,cog}$, must be expressed on the LHV basis. The worst case for the engine is that with water inlet at 70°C. For such case, PES is equal to about 17%. The best case is that with water inlet at 30°C, for which PES is 22%. These high values of PES show a remarkable advantage of the engine over conventional technology by the point of view of primary energy use.

5. Conclusions

The present work covers the experimental and numerical study of a commercial Stirling engine. External and internal measurements of three test cases are used to calibrate and validate a numerical model. This model is an extension of the well-known Urieli and Berchowitz work, applied to a specific commercial machine.

Experimental measurements at the unit boundaries are recorded to reconstruct mass and energy balances, and internal measurements on water and exhaust lines to validate the numerical model. Measured net electrical efficiency of the CHP unit is found to exceed slightly 9% (based on fuel HHV), whereas computed net electrical efficiency of the Stirling engine itself is about 15% (based on the heat input to the engine). Thermal efficiency is strongly influenced by cogeneration water inlet temperature and varies from about 90% (HHV) at 30°C inlet to about 84% at 70°C inlet. The Primary Energy Index (PES) computed accordingly to the EU Directve is always remarkably positive. The comparison of experimental and numerical data shows that maximum deviations are about 4% on net power output, whereas they remain below 1% on heat input and rejection. It is not possible to directly measure (i) mechanical frictional losses, (ii) several geometric dimensions inside the engine ducts, and (iii) the wall temperature of the heater. These parameters would allow a finest tuning of the numerical model.

Acknowledgements

The authors acknowledge gratefully the support by *Regione Lombardia*. Moreover, they thank sincerely Mr. Antonio Ravidà for his cooperation and the students Mr. Emanuele Zattoni, Ms. Flavia Belvederi and Mr. Andrea Salerno, who accomplished their graduate thesis working also on the Stirling engine tests.

References

[1] G. Valenti, A. Ravidà, A. Cacace, E. Zattoni, N. Lazzari, E. Macchi “Misure sperimentali su un motore Stirling cogenerativo per applicazione domestica”, proc. of 67° ATI congress, Trieste, Italy, 11-14 Sept 2012.

[2] S. Campanari, G. Valenti, E. Macchi, G. Lozza, A. Ravidà, N. Lazzari “Development of a microcogeneration laboratory and testing of a natural gas CHP unit based on PEM fuel cells”, proc. of 3rd Int. Conf. on Microgeneration and Related Technologies – Microgen3, Naples, 15-17 April 2013, submitted to Applied Thermal Engineering, 2013.

[3] D. Gedeon, J.G. Wood, “Oscillating-Flow Regenerator Test Rig: Hardware and Theory With Derived Correlations for Screens and Felts”, NASA Contractor Report 198442. (1996).

[4] A. A. Aliabadi, M. J. Thomson, J. S. Wallace, T. Tzanetakis, W. Lamont, J. Di Carlo “Efficiency and Emissions Measurement of a Stirling-Engine-Based Residential Microcogeneration System Run on Diesel and Biodiesel”, Energy & Fuels, vol. 23(2), pp. 1032–1039, 2009. doi:10.1021/ef800778g.

[5] N. C. J. Chen, F. P. Griffin, “A Review of Stirling Engine Mathematical Models”, Oak Ridge National Laboratory (1983)

[6] B. Cullen, J. McGovern, “Development of a theoretical decoupled Stirling cycle engine”, In: Proceedings of SEEP; (2009).

[7] T. Finkelstein, A. J. Organ, “Air Engines”, The American Society of Mechanical Engineers, New York 2001

[8] S. Schulz, F. Schwendig, “A General Simulation Model for Stirling Cycles” Gas Turbines Power 118(1), 1-7 (Jan 01, 1996) (7 pages)

[9] B. Kongtragool, S. Wongwises, “A review of solar-powered Stirling engines and low temperature differential Stirling engines”, Renewable and Sustainable Reviews 7 (2003) pp. 131-154.

[10] H. Karabulut, “Dynamic analysis of a free piston Stirling engine working with closed and open thermodynamic cycles” Renewable Energy 36 (2011) 1704e1709

[11] N. Parlak, A. Wagner, M. Elsner, H.S. Sohyan, “Thermodynamic analysis of a gamma type Stirling engine in non-ideal adiabatic conditions” Renewable Energy 34 (2009) pp. 266-273

[12] S.K. Andersen, H. Carlsen, P.G. Thomsen PG, “Control volume based modelling in one space dimension of oscillating, compressible flow in reciprocating machines” Simulation Modelling Practice and Theory 2006;14(8):1073e86

[13] Allan J. Organ, “The regenerator and the Stirling engine” London: Mechanical Engineering Publications Limited; (1997).

[14] K. Mahkamov. “Design improvements to a biomass Stirling engine using mathematical analysis and 3D CFD modeling”, J Energy Resour Technol (2006); pp. 128-203.

[15] Israel Urieli, David M. Berchowitz “Stirling Cycle Engine Analysis”, Adam Hilger Ltd, Bristol, 1984.

[16] “Directive 2012/27/EC of the European Parliament and of the Council of 25 October 2012 on energy efficiency” (substituting the previous Directive 2004/8/EC on the promotion of cogeneration), Official Journal of the European Union, L315/1, 2012.